Numerical Simulation of Exact Two-Dimensional Governing Equations for Internal Condensing Flows

Soumya A. Mitra, Ranjeeth R. Naik, and Amitabh Narain
Michigan Technological University, Houghton, Michigan, USA

Abstract: The paper outlines a two-dimensional computational methodology and presents results for laminar/laminar condensing flows inside mm-scale ducts. The methodology has been developed using MATLAB/COMSOL platform and is currently capable of simulating film-wise condensation for steady and unsteady flows. The results obtained are shown to be in agreement with an independently developed quasi-one-dimensional technique as well as a two-dimensional technique.
The newly developed code is employed here to investigate the effects of transverse gravity here on condensate motion inside a horizontal channel. The results obtained from the developed code are compared to condensing flow experiments inside a channel. The code development reported above is based on a suitable discretization approach for the explicit form of the underlying interface location. This approach is a precursor to a forthcoming approach that will solve an implicit representation of the interface location by the type of methods used in the level-set technique.

Keywords: Condensing flow simulations, interface tracking method.

1. Introduction

Accurate numerical solutions of the full governing equations are presented for steady and unsteady laminar/laminar film condensation flows inside a channel. The computational tool presented in this paper has been developed by implementing the well tested technique (see Narain et. al. [1]) of solving two-phase condensing flow problems (see [1]-[10]) as an iterative scheme using COMSOL and our own subroutines written in MATLAB. This computational tool can be directly used to investigate the issues of annular/stratified condensing flows' heat transfer rates, flow realizability, stability, noise sensitivity, and boundary condition sensitivity. Such results are important in understanding qualitative phenomena and obtaining quantitative results through suitable comparisons and synthesis with experimental results. The results obtained from the computational tool for quasi-steady annular/stratified internal condensing flows will be helpful in achieving good design and performance enhancement of condensers in thermal management systems (electronic cooling devices, etc.).

The computational methodology used in this paper, which was earlier employed on the FORTRAN platform, is well tested and has been validated by comparison with condensing flow experiments (see [3], [7], and [8]). The computational methodology has also been used to investigate classical analytical solutions for vertical (see Phan et. al. [6]) and horizontal condensing flow situations (see Kulkarni et. al. [7]). This paper presents the governing equation, computational approach and the solution scheme utilized to develop the computational tool on COMSOL.

The computational tool being developed is used here to investigate internal condensing flows inside a channel (see Fig. 1) or a tube. This tool is based on an approach ([1]-[7]) that models the interface as sharp. This is accomplished by doing separate CFD calculations for each one of the two phases on a COMSOL/MATLAB platform and doing the iterative assembly of the separate single-phase solutions in conjunction with interface tracking with the help of our own subroutines on MATLAB. For interface tracking, the reported method as well as a new approach of locating the interface by an implicit equation (by a modified level-set type solver) – but not the level-set method itself - will be used.

The paper compares the results obtained from this new tool with the results obtained from two independent computational techniques namely: the two-dimensional (2-D) technique implemented on FORTRAN platform and quasi one-dimensional technique. The 2-D technique utilizes the same computational methodology outlined in this paper, but has greater limitations compared to the COMSOL based tool. The present tool offers improvement in handling large domain size, enhanced computational speed, etc. The 1-D technique is used for computing some of the results based on an algorithm that solves the governing equations as

a set of non-linear ordinary differential equations.

The results obtained from the computational tool are compared with the condensing flow experiments of Lu and Suryanarayana [11]. The agreement between the computations and experiments validates the computational tool.

The reported computational methodology only allows the investigation of annular/stratified condensing flows because of a certain explicit representation for the interface location. The forthcoming and planned modification of the methodology to incorporate an implicit representation of the interface will allow us to investigate non-annular plug/slug, bubbly, etc. flow regimes. This capability will further the understanding of condensing flows and will help in answering unresolved issues related to transition of annular flows to non-annular flows, response of the flow to boundary condition constraints and fluctuations, heat transfer rates in these different regimes, response of the flow to changes in gravity vector, etc. These issues are particularly important in understanding the flow physics and role of boundary condition sensitivity in shear driven flows which are typically realized in horizontal channel flows, 0g flows and in micro-meter scale hydraulic diameter ducts [10].

2. Governing Equations

The two-dimensional (steady or unsteady) computational approach employed to investigate internal condensing flows in channels and tubes is based on the full governing equations described here.

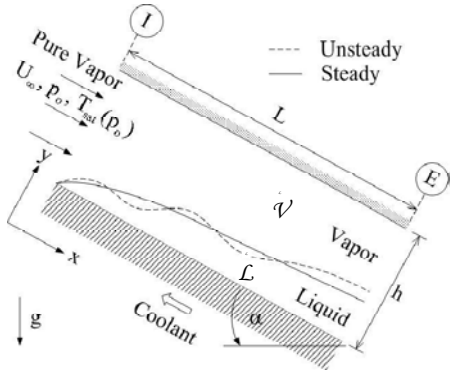

Figure 1: A schematic of a representative condensing flow problem in a channel.

The liquid and vapor phases in the flow (see Fig. 1) are denoted by $\mathcal{L}$ (subscript I: I = 1) for liquid and $\mathcal{V}$ (I = 2) for vapor. The fluid properties (density ρ, viscosity μ, specific heat C_p, and thermal conductivity k) with subscript I are assumed to take their representative constant values for each phase (I = 1 or 2). Let T_I be the temperature fields, p_I be the pressure fields, T_s (p) be the saturation temperature of the vapor as a function of local pressure p at the interface, Δ be the film thickness, $\dot{m}$ be the local interfacial mass flux, T_w (x) (< T_s (p)) be a known temperature variation of the condensing surface (with its length average mean value being $\overline{T}_W$), and $\mathbf{v}_I = u_I\hat{\mathbf{i}}+v_I\hat{\mathbf{j}}$ be the velocity fields. The flow fields are defined at every point **x** (a 3-D Euclidean position vector) and time *t*. Furthermore, the characteristic length L_c for the channel geometry is its channel gap 'h' shown in Fig. 1. Let g_x and g_y be the components of gravity along x and y axes, p_0 be the inlet pressure, $\Delta T \equiv T_s(p_0) - \overline{T}_W$ be a representative controlling temperature difference between the vapor and the bottom plate, h_{fg} be the heat of vaporization at temperature T_s (p), and U be the average inlet vapor speed determined by the inlet mass flow rate $\dot{M}_{in}$ (≡ ρ_2•U•h for the channel flow). Let t represent the actual time and (x, y) represent the physical distances of a point with respect to the axes shown in Fig. 1 for the channel flow. The line x = 0 is at the inlet, and the line y = 0 is at the condensing surface. For the channel of height 'h,' y = h is an isothermal plate and is a slightly superheated non-condensing surface. Note that, $y \equiv L_c.y$ represents the normal distance from the condensing surface. We introduce a new list of fundamental non-dimensional variables – viz. $(x, y, t, \delta, u_I, v_I, \pi_I, \theta_I, \dot{m})$ through the following definitions:

$$\{x, y, \Delta, u_I, \dot{m}\} \equiv \{L_c \cdot x, L_c \cdot y, L_c \cdot \delta, U \cdot u_I, \rho_1 \cdot U \cdot \dot{m}\}$$
$$\{v_I, T_I, p_I, t\} \equiv \{U \cdot v_I, (\Delta T) \cdot \theta_I, p_0 + \rho_1 U^2 \cdot \pi_I, (L_C / U) \cdot t\}. \quad (1)$$

Interior Equations

The non-dimensional differential forms of mass, momentum (x and y components), and energy equations for 2-D flow in the interior of either of the incompressible phases are the well-known equations:

$$\frac{\partial u_I}{\partial x} + \frac{\partial v_I}{\partial y} = 0$$

$$\frac{\partial u_l}{\partial t}+u_l\frac{\partial u_l}{\partial x}+v_l\frac{\partial u_l}{\partial y}=-\left(\frac{\partial \pi_l}{\partial x}\right)+Fr_x^{-1}+\frac{1}{Re_l}\left(\frac{\partial^2 u_l}{\partial x^2}+\frac{\partial^2 u_l}{\partial y^2}\right)$$

$$\frac{\partial v_l}{\partial t}+u_l\frac{\partial v_l}{\partial x}+v_l\frac{\partial v_l}{\partial y}=-\left(\frac{\partial \pi_l}{\partial y}\right)+Fr_y^{-1}+\frac{1}{Re_l}\left(\frac{\partial^2 v_l}{\partial x^2}+\frac{\partial^2 v_l}{\partial y^2}\right) \quad (2)$$

$$\frac{\partial \theta_l}{\partial t}+u_l\frac{\partial \theta_l}{\partial x}+v_l\frac{\partial \theta_l}{\partial y}\approx\frac{1}{Re_l Pr_l}\left(\frac{\partial^2 \theta_l}{\partial x^2}+\frac{\partial^2 \theta_l}{\partial y^2}\right),$$

where $Re_l \equiv \rho_l U\hbar/\mu_l, Pr_l \equiv \mu_l C_{pl}/k_l, Fr_x^{-1} \equiv g_x\hbar/U^2$ and $Fr_y^{-1} \equiv g_y\hbar/U^2$.

Interface Conditions

The nearly exact interface conditions for condensing flows are given in Narain et. al. [1], and Delhaye [12]. Utilizing a superscript "i" for values of flow variables at the interface $\phi \equiv y-\Delta(x,t)=0$, non-dimensional forms of the interface conditions are given below.

- The non-dimensional form of the requirement of continuity of tangential component of velocities becomes:

$$u_2^i = u_1^i - \delta_x(v_2^i - v_1^i), \quad (3)$$

where $\delta_x \equiv \partial\delta/\partial x$.

- The non-dimensional form of the normal component of momentum balance at the interface becomes:

$$\pi_1^i = \frac{\rho_2}{\rho_1}\pi_2^i - \frac{1}{We}\left(\frac{\delta_{xx}}{[1+\delta_x^2]^{3/2}}\right)+\dot{m}^2\left(\frac{\rho_1}{\rho_2}-1\right), \quad (4)$$

where $We \equiv \rho_1 U^2\hbar/\sigma$, and surface tension $\sigma = \sigma(\mathcal{T})$ where $\mathcal{T}$ is the interfacial temperature.

- The tangential component of momentum balance at the interface (see Eq. (A. 4) in Narain et al. [1]) becomes:

$$\left.\frac{\partial u_1}{\partial y}\right|^i = \frac{\mu_2}{\mu_1}\left.\frac{\partial u_2}{\partial y}\right|^i + [t], \quad (5)$$

where the term [t] in Eq. (5) is defined in Eq. (A.9) in [1].

- The non-dimensional form of non-zero interfacial mass fluxes $\dot{m}_{LK}$ and $\dot{m}_{VK}$ (defined in Eq. (A.5) of [1]) impose kinematic constraints on the interfacial values of the liquid and vapor velocity fields and are given by:

$$\dot{m}_{LK} \equiv \left[u_1^i(\partial\delta/\partial x)-(v_1^i-\partial\delta/\partial t)\right]/\sqrt{1+(\partial\delta/\partial x)^2}, \text{ and}$$
$$\dot{m}_{VK} \equiv (\rho_2/\rho_1)\left[u_2^i(\partial\delta/\partial x)-(v_2^i-\partial\delta/\partial t)\right]/\sqrt{1+(\partial\delta/\partial x)^2}. \quad (6)$$

- The non-dimensional form of non-zero interfacial mass flux $\dot{m}_{Energy}$ (as given by Eq. (A.6) of [1]) represents the constraint imposed by net energy transfer across the interface and is given by:

$$\dot{m}_{Energy} \equiv Ja/(Re_1 Pr_1)\{\partial\theta_1/\partial n\big|^i - (k_2/k_1)\partial\theta_2/\partial n\big|^i\}, \quad (7)$$

where $Ja \equiv C_{p1}\Delta\mathcal{T}/\hbar^0_{fg}$, and

$\hbar^0_{fg} \equiv \hbar_{fg}(\mathcal{T}_s(p_o)) \cong \hbar_{fg}(\mathcal{T}_s(p_2^i))$.

- The interfacial mass balance requires that the net mass flux (in kg/m^2/s) at a point on the interface, as given by Eq. (A.7) of [1], be single-valued regardless of which physical process is used to obtain it. The non-dimensional form of this requirement becomes:

$$\dot{m}_{LK} = \dot{m}_{VK} = \dot{m}_{Energy} \equiv \dot{m}. \quad (8)$$

It should be noted that negligible interfacial thermal resistance and equilibrium thermodynamics on either side of the interface is assumed to hold for x – values downstream of the origin (i.e., second or third computational cell onwards).

- The non-dimensional thermodynamic restriction on interfacial temperatures (as given by Eq. (A.8) in [1]) becomes:

$$\theta_1^i \cong \theta_2^i = \mathcal{T}_s(p_2^i)/\Delta\mathcal{T} \equiv \theta_s(\pi_2^i). \quad (9)$$

Within the vapor phase, for the refrigerants considered here, changes in absolute pressure relative to the inlet pressure are big enough to affect vapor motion but, at the same time, they are usually very small (except in micro-scale ducts) to affect saturation temperatures. Therefore, we have $\theta_s(\pi_2^i) \cong \theta_s(0)$.

Boundary Conditions

The problem posed by Eqs. (2) – (9) are computationally solved subject to the boundary conditions as shown on a representative film profile in Fig 2.

Top wall: The upper wall temperature $T_2(x, h, t) = T_{2@0} > T_{sat}(p_0)$ is at a superheated value close to saturation temperature to allow the assumption of a nearly constant saturation temperature for the vapor at all location. This is reasonable because effects of superheat (in the typical 5 – 10^{o}C range) are negligible.

Bottom wall: Besides the no-slip condition ($u_1(x, 0, t) = v_1(x, 0, t) = 0$) at the condensing surface, condensing-surface temperature ($T_1(x, 0, t) = T_w(x)$) is also prescribed, its non-dimensional form is written as

$$\theta_1(x, 0, t) = \theta_W(x) \equiv T_W(x)/\Delta T \quad (10)$$

Here Eq. (10) is known as steady temperature boundary condition for a known condensing surface temperature distribution $T_W(x)$.

Inlet Conditions: At the inlet x = 0, we have $u_2 = U$ and hence:

$$u_2(0, y, t) = 1, \ \partial v_2/\partial x\big|_{x=0} = 0. \quad (11)$$

Pressure is not prescribed across the inlet boundary but its value p_0 is specified at the corner point at the intersection of the inlet and the top wall. The inlet pressure p_{in} (= p_0) appears indirectly through important thermodynamic properties such as $h_{fg}(p_2^i) \approx h_{fg}(p_0)$ and $\mathcal{T}_{sat}(p_2^i) \approx \mathcal{T}_{sat}(p_0)$. The interfacial pressure variations are obtained from the non-dimensional computed pressures $\pi_2^i(x, y, t)$ through the relation $p_2 = p_0 + \rho_2.U^2\, \pi_2(x, \delta(x, t), t)$.

3. Computational Approach

Firstly, a sophisticated non-linear ODE based quasi one-dimensional model (see [10]) can be used to provide an initial guess of interfacial location and interfacial velocity of steady annular stratified flow in this geometry. This choice expedites convergence, but is not a necessity. Subsequently, starting from this guess, the new computational tool based on COMSOL and MATLAB subroutines is used for improving the interface location and solving condensing flow problems. The approach is similar as our currently successful CFD approach ([1]-[10]). The simulation tool locates an interface ($\phi(x, y, z, t) = 0$) by solving the interface tracking equation arising from the interface condition:

$$\dot{m}_{LK} = \dot{m}_{Energy} \qquad (12)$$

where $\dot{m}_{LK}$ is the interfacial mass-flux (kg/m^2/s) determined by the normal component of interfacial liquid velocity relative to the interfacial velocity (see eq. (A.5) of Narain et al. [1]) and $\dot{m}_{Energy}$ is the interfacial mass-flux (kg/m^2/s) determined by the interfacial energy balance (see eq. (A.6) of Narain et al. [1]) requirement associated with removal of latent heat released by the condensation rate. This requirement is rewritten in the popular interface evolution equation form:

$$\frac{\partial \boldsymbol{\varphi}}{\partial \mathbf{t}} + \mathbf{V}_{\mathbf{eff}} . \nabla \boldsymbol{\varphi} = \mathbf{0} \qquad (13)$$

where $\mathbf{V_{eff}} \equiv \mathbf{v}_1^i - (k_1 \cdot \nabla \mathcal{T}_1\big|^i - k_2 \cdot \nabla \mathcal{T}_2\big|^i) \cdot (1/\rho_1) \cdot (1/h_{fg})$ is the modified velocity determined by the vertical component of liquid interfacial velocity $\mathbf{v}_1^i$, liquid and vapor temperature gradients at the interface ($\nabla \mathcal{T}_1\big|^i$ and $\nabla \mathcal{T}_2\big|^i$ respectively), liquid density ρ_1, liquid and vapor thermal conductivities (k_1 and k_2 respectively), and the latent heat or heat of vaporization h_{fg}. The above equation is currently solved by a 2D interface tracking method valid only for ϕ explicitly given as, $y - \delta(x,t) = 0$. In the forthcoming approach, we propose the enhancement of this interface tracking method by a level-set type technique [13] for solving the above Eq. (13) without any assumption on the form of ϕ.

The proposed approach is different than the approach in other level-set techniques [14]-[17] on three counts: (i) the "interface" is to be modeled as "sharp" instead of the more common "thin zone" models used for level set simulations, (ii) the liquid and vapor domains are to be solved separately and consecutively as opposed to concurrent solving of both the domains, and (iii) the original hyperbolic nature of the interface tracking equation will be retained as opposed to tweaking of this equation with diffusive terms for computational convenience (see [18]).

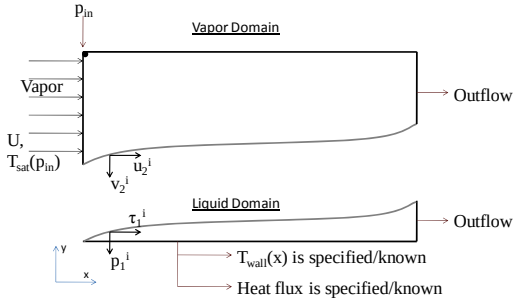

Figure 2: For a representative film profile the figure shows the boundary conditions for each liquid and vapor domain.

The computational tool development is based on the solution algorithm described below:

I. The guess of film thickness, interfacial velocities for the liquid domain, and interfacial mass flux obtained from the 1D simulation are used to compute the interfacial vapor velocities through "functions" in COMSOL/MATLAB. Steady and unsteady simulations uses one of the *interfacial mass-flux conditions* ($\dot{m}_{VK} = \dot{m}_{Energy}$) and the *continuity of tangential velocity* (Eq.3) to obtain the normal and tangential components of the interfacial vapor velocity from the guessed values of liquid interfacial velocities. For the steady equations, the time derivatives in these equations are set to zero.

II. From the interfacial values of the vapor velocities obtained above, the CFD solution

for the vapor domain (marked $\mathcal{V}$ in Fig. 1) is implemented on the COMSOL/MATLAB platform based on the boundary conditions discussed in section 2 and depicted in Fig. 2. The interface location is used to create and mesh the vapor domain in Fig. 2 with the help of ALE ("Arbitrary Lagrangian - Eulerian") method [19] available on COMSOL. This ALE method is an effective moving boundary/mesh method for these types of problems.

III. The necessary information from the vapor domain solution is extracted and transferred to the liquid domain such that the normal and tangential stress τ_1^i and p_1^i shown in Fig. 2 are obtained with the help of Eq. (4) and Eq. (5). The momentum and continuity equations for the liquid domain (marked $\mathcal{L}$ in Fig. 1) is solved on COMSOL platform for the chosen guess of the interface location (same as that in vapor domain calculation). This is done by prescribing the boundary conditions – which are "normal (pressure) and tangential (shear) stress conditions" at the interface, an "outflow" at the exit, and wall conditions at the condensing surface based on the nature of heating/cooling as shown in Fig. 2. The results presented in this paper are for prescribed saturation temperature condition at the interface and prescribed wall temperature at the condensing surface. Again, ALE method is used to create and mesh the liquid domain in Fig. 2.

IV. The initial values for the interface location (ϕ ($\mathbf{x}$, t) = 0) at t = nΔt, n = 0, 1, 2, etc. are used to predict the interface location at discrete values of t = (n+1)Δt and $\mathbf{x} \equiv x\mathbf{i} + y\mathbf{j} + z\mathbf{k}$. This is currently done through the interface tracking approach (see [1]) used by us.

Furthermore, the choice of the grid for tracking the interface is such that it satisfies, as in [1], the Courant number restriction ($Cr_x \approx 1$, $Cr_y \approx 1$ and $Cr_z \approx 1$), allowing accurate resolution of wave amplitudes and their phase angles even for relatively coarse grids. This alternative discretization makes the solution scheme verifiably compatible with analytically obtained "method of characteristics" approaches.

V. After obtaining *tentative* new interface locations for time t = (n + 1)Δt as described above, each domain in the steps II and III is updated for the this new interface boundary with the help ALE method which moves the existing mesh inside the domain to conform to the new interface locations ($\mathcal{L}_t \rightarrow \mathcal{L}_{t+\Delta t}$ and $\mathcal{V}_t \rightarrow \mathcal{V}_{t+\Delta t}$) and creates new geometries from the moved meshes, namely $\mathcal{L}_{t+\Delta t}$ and $\mathcal{V}_{t+\Delta t}$. The ALE method is also used to remap the flow field values in the interiors and at the interface of $\mathcal{L}_t$ and $\mathcal{V}_t$ to the interiors and at the interface of $\mathcal{L}_{t+\Delta t}$ and $\mathcal{V}_{t+\Delta t}$ respectively.

VI. The above sequence of steps I-IV is repeated at each time until a good estimate of the interface location at t = (n+1)Δt is obtained in step III. This also means that the effective velocity $\mathbf{v_{eff}}$ used in the interface tracking equation has been converged.

VII. Repetition of the steps I to V above will yield converged interface locations and CFD solutions for each domain at each t = nΔt for n = 1, 2, etc.

In forthcoming simulations, we will replace the current method of interface tracking by the proposed "level-set" type method. The "level-set" interface tracking equation is of the type given in Eq. (13).

4. Results and Discussion

4.1 Results and Their Comparison with Results Obtained from Other Computational Tools

The algorithm outlined in this paper yields steady as well as unsteady condensing flow results for different values of g_x and g_y shown in Fig. 1. These solutions are compared with other computational techniques as well as experimental results. Figure 3 compares the steady film thickness solutions obtained from this computational tool with those obtained from the other computational tools (namely, 1D and 2D FORTRAN code). These tools (1D and 2D FORTRAN code) are validated by comparing with experimental results as well as comparing with analytical solutions.

The steady solution obtained by the COMSOL tool agrees with the solution obtained by the 1D and the 2D FORTRAN codes. Even though the agreement shown in Fig. 3 is for the film thickness values, all other flow variables are also in good agreement but are not shown here for brevity. In Fig. 3, the initial guesses used for the simulation are 0.9 and 0.95 times the 1-D

steady solution. The same steady solution is achieved by using different initial guesses of film thickness (as shown in Fig. 3) and/or different initial guess for interfacial velocities. Even though the algorithm used to obtain these results is robust, it is recommended to use the 1D steady solution as an initial guess for these problems, as it reduces computational time by expediting convergence.

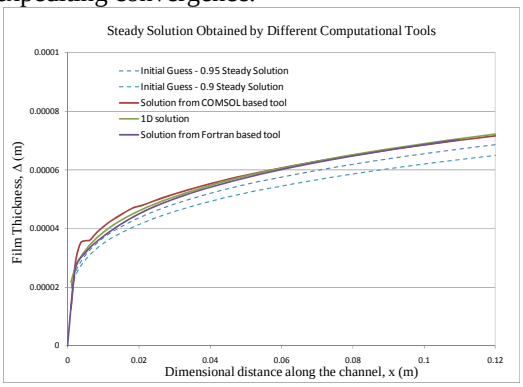

Figure 3: For a flow of pure R113 vapor with average inlet vapor speed of 0.41 m/s and vapor to condensing surface temperature difference of 5 °C, the figure shows the agreement in film thickness values that are obtained from COMSOL based computational tool, 1D tool [10] and 2D FORTRAN tool [1]. The figure also shows the solution of the COMSOL based computational tool remain the same for two different initial guesses.

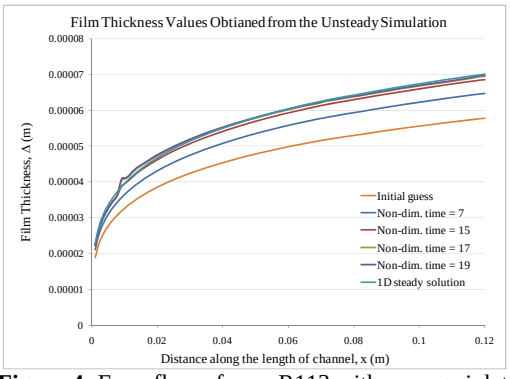

Figure 4: For a flow of pure R113 with average inlet vapor speed = 0.8 m/s and vapor to condensing surface temperature difference of 5 °C, the figure shows the time evolution of the liquid vapor interface with time. The film thickness value for long term solution ($t \rightarrow \infty$) agrees with the steady solution obtained from the COMSOL tool as well as the 1D solution technique.

The solutions shown in Fig. 4 show the time evolution of the liquid-vapor interface (film) if the initial guess of the film is away from the steady solution. It is shown that the long term ($t \rightarrow \infty$) solution of the unsteady equations is same as the solution obtained from the steady equations. The computational tool presented here can be used to simulate the response of the condensing flow to initial disturbance, bottom wall vibrations, inlet or outlet pressure fluctuations as well as mass flow rate fluctuations, and changes in thermal boundary conditions. These additional results are not shown here for brevity but will be discussed in forthcoming publications.

4.2 Comparison with Experimental Results

In [10], it is shown that the horizontal channel condensing flow experiments with R113 vapor by Lu and Suryanarayana [11] have an inclination of around 1°. Therefore, the results obtained from the computational tool using COMSOL were compared with the channel flow experiments with 1° tilt. Figure 5 shows a comparison of the film thickness values measured during a channel flow experiments (Run 213) of Lu and Suryanarayana [11] with the solution obtained from the computational tool. The experiments measure the film thickness at 5 different locations shown in Fig. 5. It is seen that the film thickness profile obtained from the simulation is in agreement (within experimental error) with the experimental results. Equally good comparisons for several cases of the channel flow experiments of Lu and Suryanarayana [11] are shown in Table 1.

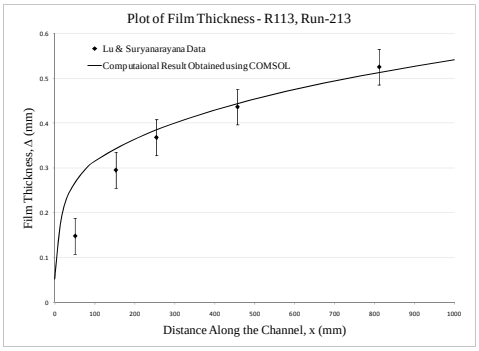

Figure 5: For the flow of R113 in a channel with average inlet speed of 1.11 m/s and saturation to condensing surface temperature difference of 21.2 °C, the figure shows the film thickness profile obtained by the computational tool using COMSOL. These film thickness values are compared with the film thickness values (and associated error bars) obtained by the Lu and Suryanarayana [11] experiments.

Table 1. Comparison of film thickness values from Lu & Suryanarayana [11] experimental results with the results from the computational tool based on COMSOL.

Comparison of Lu & Suryanarayana Experimental data with Computaional Results for R113 with an Inclination of 1 degree														
Run	Fluid	U	Delta_T	Film Thickness Experimental,mm					Film Thickness Computaional, mm					Error between Exp
		m/s	°C	50.8	152.4	254	457.2	812.2	50.8	152.4	254	457.2	812.2	and Comp (%)
208	R-113	0.861764	22.28	0.147	0.296	0.344	0.37	0.4	0.226	0.298	0.339	0.394	0.456	9.1
211	R-113	1.10659	21.2	0.134	0.271	0.298	0.368	0.397	0.218	0.290	0.331	0.386	0.449	12.3
223	R-113	1.256109	37.03	0.165	0.294	0.358	0.423	0.504	0.253	0.333	0.378	0.438	0.505	8.5
213	R-113	1.281019	39.73	0.148	0.295	0.368	0.436	0.525	0.257	0.338	0.384	0.445	0.514	8.6
215	R-113	1.277654	21.65	0.106	0.195	0.247	0.345	0.38	0.219	0.289	0.328	0.381	0.440	23.2
206	R-113	1.710475	30.95	0.17	0.28	0.34	0.375	0.412	0.236	0.309	0.350	0.405	0.466	10.7

5. Conclusions

- An algorithm for successful and accurate computational simulations of steady and unsteady condensing flows has been presented.
- The results from the computational tool using COMSOL are in good agreement with the 2-D computational code based on FORTRAN and a completely independent quasi 1-D tool.
- Relevant results from the reported computational tool developed here are shown to be in agreement with the experimental results for the inclined channel flow experiments.
- Besides the reported successful implementation of the current algorithm for simulating film-wise condensation, modifications in the algorithm are planned that will allow an implicit representation of the interface location which in turn will allow us to simulate plug/slug ,bubbly, etc. flow regimes as well.

6. References

1. A. Narain, Q. Liang, G. Yu, X. Wang, Direct Computational Simulations for Internal Condensing Flows and Results on Attainability/Stability of Steady Solutions, Their Intrinsic Waviness, and Their Noise-Sensitivity, Journal of Applied Mechanics, 71 (2004) pp. 69-88.
2. A. Narain, S. D. Kulkarni, S. Mitra, J. H. Kurita, M. Kivisalu, Computational and Ground Based Experimental Investigations of the Effects of Specified and Unspecified (Free) Pressure Conditions at Condenser Exit for Condensing Flows in Terrestrial and Micro-Gravity Environments, Annals of New York Academy of Sciences, Interdisciplinary Transport Phenomenon, 2008.
3. A. Narain, J. H. Kurita, M. Kivisalu, S. D. Kulkarni, A. Siemionko, T. W. Ng, N. Kim, L. Phan, Internal Condensing Flows Inside a Vertical Pipe – Experimental/Computational Investigations of the Effects of Specified and Unspecified (Free) Conditions at Exit, ASME Journal of Heat Transfer (2007) pp. 1352-1372.
4. Q. Liang, X. Wang, and A. Narain, Effect of Gravity, Shear and Surface Tension in Internal Condensing Flows - Results from Direct Computational Simulations, ASME Journal of Heat Transfer 126 (5) (2004), pp. 676-686.
5. L. Phan, X. Wang, A. Narain, Exit Condition, Gravity, and Surface-Tension Effects on Stability and Noise-sensitivity Issues for Steady Condensing Flows inside Tubes and Channels, International Journal of Heat and Mass Transfer 49 Issues 13-14 (2006) pp. 2058-2076.
6. L. Phan, A. Narain, Non-linear Stability of the Classical Nusselt Problem of Film Condensation and Wave-Effects, ASME Journal of Applied Mechanics 74 (2) (2007), pp. 279-290.
7. S. D. Kulkarni, A. Narain, and S. Mitra, Forced Flow of Vapor Condensing over a Horizontal Plate (Problem of Cess and Koh*) – Steady and Unsteady Solutions of the Full 2D Problem, Accepted for publication in ASME Journal of Heat Transfer, Vol. 132, pp. 101502-1 – 18, Oct (2010). Also see: http://www.me.mtu.edu/~narain.
8. J. H. Kurita, M. Kivisalu, S. Mitra, A. Narain, Experimental Results on Gravity Driven Condensing Flows in Vertical Tubes, their Agreement with Theory, and their Differences with Shear Driven Flows' Boundary Condition Sensitivities, Submitted to International Journal of Heat and Mass Transfer, (2010).
9. S. D. Kulkarni, A. Narain, S. Mitra, J. H. Kurita, M. Kivisalu, M. M. Hasan, Flow Control and Heat Transfer Enhancement

Issues Resulting from Elliptic Sensitivity for Shear Driven Annular/Stratified Internal Condensing Flows, Submitted for publication in the Journal of Transport Processes.
10. S. Mitra, A. Narain, R. Naik, S.D. Kulkarni, Quasi One-dimensional Theory for Shear and Gravity Driven Condensing Flows and their Agreement with Two-dimensional Theory and Selected Experiments, submitted for publication in the Int. J. of Heat and Mass Transfer, (2010).
11. Q. Lu, N. V. Suryanarayana, Condensation of a vapor flowing inside a horizontal rectangular duct, Journal of Heat Transfer 117 (1995), pp. 418-424.
12. Delhaye, J. M., 1974, "Jump Conditions and Entropy Sources in Two-phase Systems; Local Instant Formulation," *Int. J. of Multiphase Flow*, **1**, pp. 395-409.
13. S. Osher, R. Fedkiw, "Level Set Methods and Dynamic Implicit Surfaces," Springer-Verlag New York,Applied Mathematical Sciences, 153, 2002.
14. Son, G. and V. K. Dhir, 1998, "Numerical Simulation of Film Boiling Near Critical Pressures with a Level Set Method," *Journal of Heat Transfer* 120, pp. 183-192.
15. Mukherjee, A. and V. K. Dhir, 2005, "Study of Lateral Merger of Vapor Bubbles During Nucleate Pool Boiling," Journal of Heat Transfer, Vol. 126, pp. 1023-1039.
16. Sussman, M., P. Smereka, and S. Osher, 1994 "A Level Set Approach for Computing Solutions to Incompressible Two-Phase Flow," *J. of Comput. Phys.*, Vol. 114, pp. 146-159.
17. Enright, D., R. Fedkiw, J. Ferziger, and I. Mitchell, 2002, "A Hybrid Particle Level Set Method for Improved Interface Capturing," *Journal of Computational Physics*, volume 183, number 1, pp. 83-116.
18. Gibou, F., L. Chen, D. Nguyen, and S. Banerjee, 2007, "A Level Set Based Sharp Interface Method for the Multiphase Incompressible Navier-Stokes Equations with Phase Change," *Journal of Computational Physics*, vol. 222, pp. 536-555.
19. "Multiphase Flow-Boiling Flow" Chapter 6, Model Library, Chemical Engineering Module, COMSOL MULTIPHYSICS by COMSOL Inc., pp. 255-269.

7. Acknowledgements

This work is supported by NASA grant NNX10AJ59G and NSF grant NSF-CBET-1033591.